

# Simultaneous spatial and temporal walk-off compensation in frequency-doubling femtosecond pulses in $\beta$ -BaB<sub>2</sub>O<sub>4</sub>

Russell J. Gehr, Mark W. Kimmel, and A. V. Smith

Department 1128 Lasers, Optics and Remote Sensing, Sandia National Laboratories, Albuquerque, New Mexico 87185-1423

Received May 12, 1998

We experimentally demonstrate the benefits of simultaneous compensation of spatial and temporal walk-off in frequency doubling of 800-nm 250-fs pulses, using three active and two compensating  $\beta$ -BaB<sub>2</sub>O<sub>4</sub> crystals. The compensating crystals reverse both birefringent and group-velocity walk-off, resulting in a factor-of-4.5 improvement in doubling efficiency relative to one of the active crystals while maintaining the short pulse duration and the symmetric spatial profile that are characteristic of the single crystal. © 1998 Optical Society of America

OCIS codes: 320.7110, 190.2620, 190.7110.

Frequency doubling in nonlinear crystals is usually subject to limitations imposed by birefringent and group-velocity walk-off. These effects are discussed in Ref. 1 and the references therein. Briefly, birefringence causes lateral walk-off between the interacting beams. The angle  $\rho$  between the propagation and the Poynting vectors of a beam is given by

$$\rho = \frac{-1}{n(\theta)} \frac{dn(\theta)}{d\theta} \quad (1)$$

and is typically a few tens of milliradians for extraordinary- (*e*-) polarized beams or zero for ordinary- (*o*-) polarized beams. Critical phase matching involves both *e* and *o* waves, so there is always some spatial separation of the beams as they propagate through the crystal. This separation can reduce mixing efficiency and distort the spatial profile of the product beam. Likewise, differences in the group velocities  $v$  cause two pulses with different polarization and (or) frequency to separate in time by an amount  $\sigma L$ , where  $L$  is the crystal length and  $\sigma$  depends on the group-velocity mismatch according to

$$\sigma = \frac{1}{v_1} - \frac{1}{v_2}, \quad (2)$$

which also reduces the mixing efficiency and can stretch the product pulse in time.

As numerous authors have pointed out,<sup>1</sup> one can minimize lateral walk-off by stacking multiple crystals with alternating walk-off directions. Similarly, temporal walk-off compensation in crystal stacks with alternating signs of group-velocity walk-off has been discussed<sup>1,2</sup> but to our knowledge has not been demonstrated in the laboratory. Here we present laboratory measurements of simultaneous lateral and temporal walk-off compensation in type I frequency doubling of 250-fs 800-nm pulses in  $\beta$ -BaB<sub>2</sub>O<sub>4</sub> crystals. This process is phase matched at  $\theta = 29.2^\circ$  with a lateral walk-off between the fundamental and the second harmonic of  $68 \mu\text{m}/\text{mm}$  and a group-velocity walk-off of  $194 \text{ fs}/\text{mm}$ . At the non-phase-matching angle of  $70.4^\circ$ , the ratio of lateral to temporal walk-off

has the same magnitude, but temporal walk-off has the opposite sign. Lateral walk-off is  $45.7 \mu\text{m}/\text{mm}$ , and group-velocity walk-off is  $-129 \text{ fs}/\text{mm}$ . By alternating non-phase-matched, or passive,  $70.4^\circ$  crystals of length  $1.5 L$ , with phase-matched, or active, crystals of length  $L$ , oriented with alternating lateral walk-off direction, we simultaneously compensate for lateral and temporal walk-off. We used the arrangement shown in Fig. 1 for our demonstration, with three active crystals and two passive compensating crystals.

Before presenting our results, we note for completeness that other means of matching the group velocities of two waves, such as the use of slanted pulses<sup>3</sup> in collinear mixing, wherein lateral walk-off combines with slanted spatial profiles to compensate for group-velocity differences, have been demonstrated. Viewed in terms of wave vectors and frequencies,  $(\mathbf{k}, \omega)$ , rather than the space and time variables,  $(\mathbf{r}, t)$ , this approach is called achromatic phase matching,<sup>4</sup> in which each frequency component of the input beam is tilted to its phase-matching angle, using gratings and (or) prisms, perhaps in conjunction with imaging lenses. The slant of the output pulses can be removed, again by use

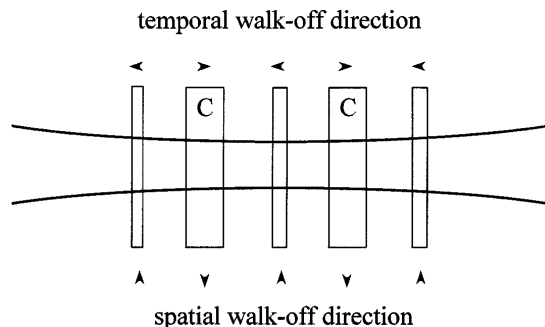


Fig. 1. Diagram of the crystal arrangement. The crystals labeled C are the inactive compensation segments. The others are the active crystal segments. Both temporal and spatial walk-off are opposite in the compensating and the active segments. The arrows indicate the direction that the *e*-polarized second-harmonic pulse shifts with respect to the *o*-polarized fundamental pulse in our experimental setup.

of dispersive optics. Matching three group velocities should be possible by combination of noncollinear mixing with slanted pulses. Although this mixing apparently has not been demonstrated, various noncollinear mixing experiments have been reported in which two group velocities were matched.<sup>5</sup> Matching the group velocities of the signal and idler pulses in optical parametric amplification is sufficient to give broad spectral gain bandwidths with a long pump pulse, permitting chirped-pulse amplification and, with compression, short signal and idler pulses. These methods have proven effective for many applications, but complications of beam conditioning and correction with prisms and gratings, wavelength-dependent output beam angles, and narrow angular acceptance, or equivalently, large spatial walk-off, can limit their use, particularly in mixing weak pulses. Our method minimizes the beam-conditioning optics while retaining the angular and the spectral acceptance of the shorter crystal segments, albeit at the cost of having to use more crystals, with their extra surfaces and associated alignment mechanisms.

Our experimental setup is shown in Fig. 2. A Ti:sapphire laser produces 250-fs, 2- $\mu$ J pulses at 800 nm with a pulse rate of 250 kHz. The laser output is split into two beams. We use one beam (10% of the energy) to pump the doubling crystals. This beam is spatially filtered and focused to a 230- $\mu$ m-diameter spot, resulting in a confocal parameter of 10.4 cm in air. This length is sufficient to contain all three doubling crystals, plus the two compensating crystals. After passing through the doubler, the beam is recollimated and spectrally filtered so that only the 400-nm light is passed. Three 1-mm-long active crystals and two 1.5-mm-long compensating crystals are individually mounted so the position and the angle of each can be adjusted independently. The crystals are antireflection coated for 800 and 400 nm. Alignment of the crystals is accomplished iteratively: The first doubler is inserted at the 800-nm focus and aligned for optimum output power. Then a second doubler is inserted upstream and aligned with the first, followed by an intervening compensating crystal. All crystals are separated by 1 cm. The angle of this compensating crystal must be carefully adjusted because it sets the phase difference between the fundamental and the harmonic at the following active crystal. Finally, the third doubler and its compensator are inserted downstream and aligned, after which all of the crystal orientations are fine adjusted once more so that optimum power is obtained. Typically this final adjustment makes only a small difference in the total output power. In such a chain of crystals the tilt sensitivity of each is one to two times that of a single crystal with the same length as a single segment.<sup>1</sup>

We tested several arrangements of crystals: a single active crystal; two active crystals with and without a compensating crystal between them; and three active crystals with and without interspersed compensating crystals. First we measured spatial profiles of the harmonic beam, using a CCD camera and beam-profiling software. As expected, it was possible to generate high-quality spatial profiles with and

without the compensating crystals. Without compensating crystals, the active crystals were oriented with alternating lateral walk-off directions. With compensating crystals, the active doubling crystals were oriented with lateral walk-offs in the same direction but with the compensating crystals' providing opposite lateral walk-off. Of course, without lateral walk-off compensation, the spatial profiles were significantly distorted. We then measured doubling efficiencies for each crystal arrangement that produced a good spatial profile. For 9.5 mW of fundamental power, a single doubling crystal generated an average output power of 0.7 mW. For two crystals without a compensating crystal the average output power was 1.5 mW. This approximately linear scaling is anticipated because the temporal walk-off in a single crystal (194 fs) is nearly equal to the pulse length (250 fs).<sup>1</sup> Inserting the compensating crystal boosts the average output power to 2.0 mW. In the low conversion limit, with collimated beams and with no losses, we would expect the power to increase by nearly a factor of 4 in going from a single active crystal to two active crystals with compensation. The observed enhancement of 2.8 falls short of this, in part because the second crystal is displaced from the focus so the 800-nm beam is slightly larger, and in part because of a wedge in the compensator crystal of  $\sim 0.12^\circ$ , which prevents perfect phasing of the fundamental and the harmonic across the full beam at the second doubling crystal. Further improvement was found with three active crystals: Without compensating crystals the average output power was 2.2 mW, again nearly linear in active crystal length, whereas with the compensating crystals it was 3.2 mW. This increase relative to a single crystal by a factor of 4.5 is somewhat less than the factor of 6.7 estimated when we take into account depletion of the fundamental; again this is attributed to compensator wedge and displacement from the focal point.

Besides improving doubling efficiency, the compensated stack should generate shorter pulses, comparable in duration with the fundamental pulses. We measured pulse profiles for both the fundamental and the harmonic pulses. The strong fundamental beam (90% of the energy) was spatially filtered and mixed with the harmonic pulse in a 0.2-mm-thick BBO crystal cut at  $\theta = 42^\circ$  for type II difference-frequency mixing. A motorized translation stage

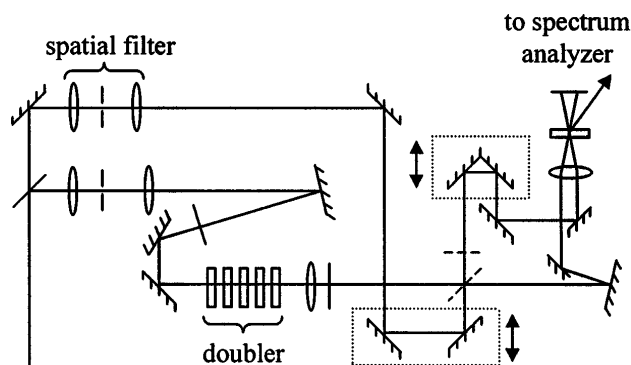


Fig. 2. Experimental setup.

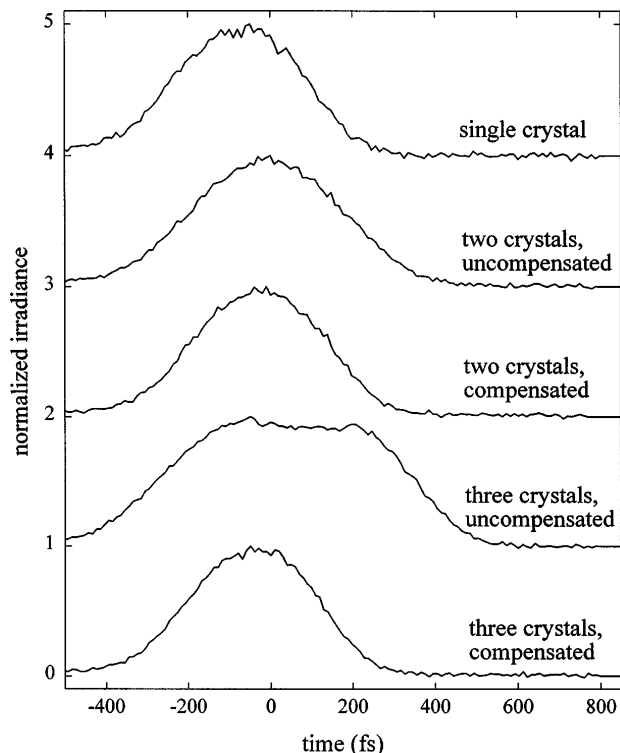


Fig. 3. Integrated FROG signal,  $I_F(\tau)$  for various arrangements of active and compensating crystals.

varied the time delay between the reference and the harmonic pulses, and we spectrally analyzed the generated difference-frequency light to generate data for frequency-resolved optical gating<sup>6</sup> (FROG). Alternatively, we could block the harmonic beam and insert a 50/50 beam splitter and a half-wave plate (indicated in Fig. 2 by the dashed lines) into the fundamental beam to produce second-harmonic generation FROG data, permitting complete characterization of the fundamental pulses. A typical fundamental pump pulse with the laser amplifier pulse compressor optimized for minimum autocorrelation duration had a FWHM of 250 fs with negligible phase distortion. Using the retrieved fundamental irradiance and the difference-frequency FROG data, we extracted the harmonic irradiance. The FROG data were first integrated over frequency, so they were related to the harmonic irradiance through a convolution of the field irradiances:

$$I_F(\tau) = \int_{-\infty}^{\infty} I_{\text{FROG}}(\omega, \tau) d\omega = \int_{-\infty}^{\infty} I_{2\omega}(t) I_{\omega}(t - \tau) dt. \quad (3)$$

These data are shown in Fig. 3. Note that the compensated stacks produce pulse widths comparable with that of a single crystal, whereas the uncompensated stacks produce noticeably longer durations. We extracted  $I_{2\omega}(t)$  from Eq. (3), using Fourier-transform methods. Because the data were noisy we used optimal filtering techniques<sup>7</sup> to obtain the pulses. Even

with filtering the noise imposed small distortions on the retrieved pulses. Therefore the retrieved second-harmonic irradiance,  $I_{2\omega}(t)$ , was checked for accuracy in two ways. First, it was inserted into the right-hand side of Eq. (3), and the resulting convolution was compared with the measured FROG data. Second, the duration of the retrieved pulse was compared with that determined by assumption of a Gaussian second-harmonic pulse shape. Typically the difference in pulse length determined by these two methods was less than 5%. The single crystal and the three crystals with compensators produced almost the same pulse duration,  $308 \pm 10$  fs and  $300 \pm 10$  fs, respectively, whereas the uncompensated arrangement produced pulses with twice this duration,  $616 \pm 10$  fs. We conclude that the compensators worked as expected; they compensated for both spatial and temporal walk-off, producing pulses with higher energies and excellent spatial and temporal profiles.

Our method of simultaneously compensating for group and birefringent walk-off should be applicable to many situations that suffer from walk-off between an  $e$  and an  $o$  wave. In general, mixing involves three waves, each with a different group velocity and birefringence. Often, however, the group velocities and lateral walk-offs of the  $e$  waves are closely spaced but quite different from those of the also closely spaced  $o$  waves, so although perfect compensation of all three waves is not possible, this method can still provide a useful degree of compensation.

This work was supported by the U.S. Department of Energy under contract DE-AC04-94AL85000. Sandia is a multiprogram laboratory operated by Sandia Corporation, a Lockheed Martin Company, for the U.S. Department of Energy.

## References

1. A. V. Smith, D. J. Armstrong, and W. J. Alford, *J. Opt. Soc. Am. B* **15**, 122 (1998).
2. T. Zhang and M. Yonemura, *Appl. Opt.* **37**, 1647 (1998).
3. R. Danielius, A. Piskarskas, P. Di Trapani, A. Andreoni, C. Solcia, and P. Foggi, *IEEE J. Quantum Electron.* **34**, 459 (1998).
4. B. A. Richman, S. E. Bisson, R. Trebino, E. Sidick, and A. Jacobson, *Opt. Lett.* **23**, 497 (1998).
5. G. Cerullo, M. Nisoli, and S. De Silvestri, *Appl. Phys. Lett.* **71**, 3616 (1997); C. Radzewicz, Y. B. Band, G. W. Pearson, and J. S. Krasinski, *Opt. Commun.* **117**, 295 (1995); A. Shirakawa and T. Kobayashi, *Appl. Phys. Lett.* **72**, 147 (1998); P. Di Trapani, A. Andreoni, C. Solcia, P. Foggi, R. Danielius, A. Dubietis, and A. Piskarskas, *J. Opt. Soc. Am. B* **12**, 2237 (1995); T. Wilhelm, J. Piel, and E. Riedle, *Opt. Lett.* **22**, 1494 (1997).
6. R. Trebino, K. W. DeLong, D. N. Fittinghoff, J. N. Sweetser, M. A. Krumbügel, B. A. Richman, and D. J. Kane, *Rev. Sci. Instrum.* **68**, 3277 (1997).
7. W. H. Press, S. A. Teukolsky, W. T. Vetterling, and B. P. Flannery, *Numerical Recipes in C* (Cambridge University, New York, 1992), pp. 547–549.